

Perylene-cored Star-shaped Polycations for Fluorescent Gene Vectors and Bioimaging

Shusen You,[†] Qing Cai,[†] Yang Zheng,[‡] Bicheng He,[‡] Jie Shen,^{*,‡} Wantai Yang,[†] and Meizhen Yin^{*,†}

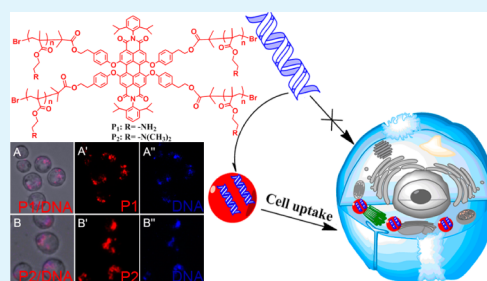
[†]State Key Laboratory of Chemical Resource Engineering, Key Laboratory of Carbon Fiber and Functional Polymers, Ministry of Education, Beijing Laboratory of Biomedical Materials, Beijing University of Chemical Technology, 100029 Beijing, China

[‡]Department of Entomology, China Agricultural University, 100193 Beijing, China

S Supporting Information

ABSTRACT: Two star polycations, poly(2-aminoethyl methacrylate) (PAEMA, **P1**) and poly(2-(dimethylamino)ethyl methacrylate) (PDMAEMA, **P2**), have been synthesized with perylene diimide (PDI) as the central fluorophore. ¹H NMR and ¹³C NMR are used to confirm the successful synthesis of a macromolecular initiator. Using ATRP strategy, **P1** and **P2** are obtained with narrow molecular weight distribution. The star polymers have good fluorescence properties in aqueous solution, which provides fluorescent tracing and imaging during gene delivery. Both **P1** and **P2** can efficiently condense DNA into stable nanoparticles. Transfection studies demonstrate that **P1** and **P2** deliver DNA into live cells with higher efficiency and lower cytotoxicity than polyethylenimine (PEI, 25 kDa). **P2** shows higher capacity for gene delivery than **P1** due to its better buffering and faster rate of cellular internalization.

KEYWORDS: star polymer, gene vector, fluorescence, bioimaging



INTRODUCTION

Perylene diimide (PDI) is an excellent fluorophore, which exhibits exceptional chemical, thermal, and photochemical stability with high fluorescence quantum yields in organic solvents.^{1–3} Due to the rigid structure of the fluorophores, they tend to aggregate and exhibit weak fluorescence in aqueous solution.⁴ To improve the solubility in water, PDIs have been modified with sulfo,^{5–7} piperazin,⁷ or polyglycerol (PG).⁸ Various fluorescent inorganic nanoparticles such as semiconductor quantum dots, photoluminescent silicon nanoparticles, and metallic nanoclusters have been synthesized and extensively investigated for biomedical applications over the past decades for many diagnostic assays.^{9–12} Among them, organic nanoparticles have also been studied in this field. Recently, water-soluble PDIs modified with dendrimers or dendritic macromolecules^{13,14} have been reported for the applications of bioimaging,^{15,16} biolabeling,^{17,18} and gene delivery.^{19,20} The synthesis approaches of star polymers with similar controlled structures are easier than those of dendrimers or dendritic macromolecules. Star polymers consist of a number of linear polymer arms joined together by a central core.^{21–23} Star polymers can be prepared through controlled/living radical polymerization methods such as atom transfer radical polymerization (ATRP).²⁴ Compared with the linear analogues, the star polymers have a high density of functional groups. Meanwhile, the star polymers can approach the topological complexity and chemical properties of dendrimers with a single key step.^{25,26} Therefore, star polymers are good candidates for mass production of functional polymers.

Gene therapy has brought us the hope of curing cancers.^{27–30} The in-depth clinical studies need gene vectors with high efficiency. Cationic polymers as a type of nonviral vectors have attracted more and more interest due to their high level of safety and ease of preparation.^{31–33} Among the cationic polymers, poly(2-aminoethyl methacrylate) (PAEMA) and poly(2-(dimethylamino)ethyl methacrylate) (PDMAEMA) with linear topology have been studied and used for gene delivery.^{12,34,35}

Herein, we designed and synthesized two star-shaped cationic polymers, **P1** and **P2**, with PDI as the central fluorophore (Schemes 1 and 2). The outer polymer arms of PAEMA or PDMAEMA provide water solubility and positive charges. Through electrostatic interaction, the PDI-cored star polycations can bind and condense nucleic acids into stable complexes. Complex formation can protect the gene from degradation and mediate cellular internalization of the gene. Both **P1** and **P2** showed lower cytotoxicity as well as higher gene delivery efficacy than PEI (25 kDa). **P2** is more suitable than **P1** as a gene vector because of its better buffering and faster cellular uptake.

EXPERIMENTAL SECTION

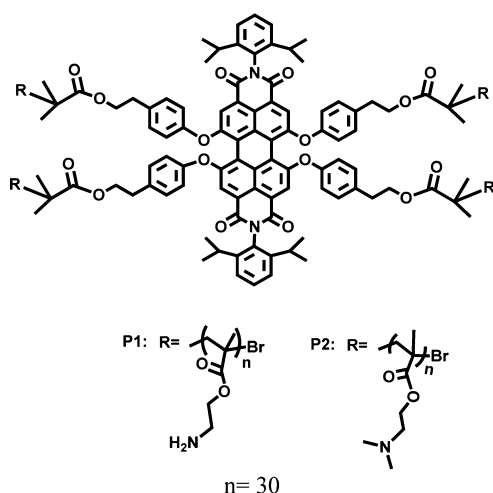
Materials. *N,N,N',N',N''*-Pentamethyldiethylenetriamine (PMDETA, 98%, Alfa Aesar), 4,4'-di-*tert*-butyl-2,2'-bipyridine (DTB-bipy, 98%, Alfa Aesar), and CuBr (99.999%, Alfa Aesar) were used as

Received: July 14, 2014

Accepted: August 27, 2014

Published: August 27, 2014

Scheme 1. Structures of (PAEMA, P1) and (PDMAEMA, P2)



obtained. 2-Butanone (99%, Acros) and 2-(dimethylamino)ethyl methacrylate (DMAEMA, 99%, Acros) were distilled under a vacuum before use. *N,N'*-Bis(2,6-diisopropylphenyl)-1,6,7,12-tetra[4-(2-hydroxyethyl) phenoxy]perylene-3,4,9,10-tetracarboxylic acid diimide (**1**) and 2-[(*tert*-butoxycarbonyl) amino] ethyl methacrylate (Boc-AEMA) were synthesized according to the previous report.^{14,36} A solution of calf ThyMus-DNA (CT-DNA) in phosphate buffer (10 mM, pH 7.4) containing 50 mM NaCl was stored at 4 °C and used after no more than 4 days. All other chemicals were used as received. S2 cells were propagated in Schneider Drosophila Medium supplemented with 10% fetal bovine serum (FBS), 100 U/mL penicillin, and 100 mg/mL streptomycin at 25 °C without CO₂.

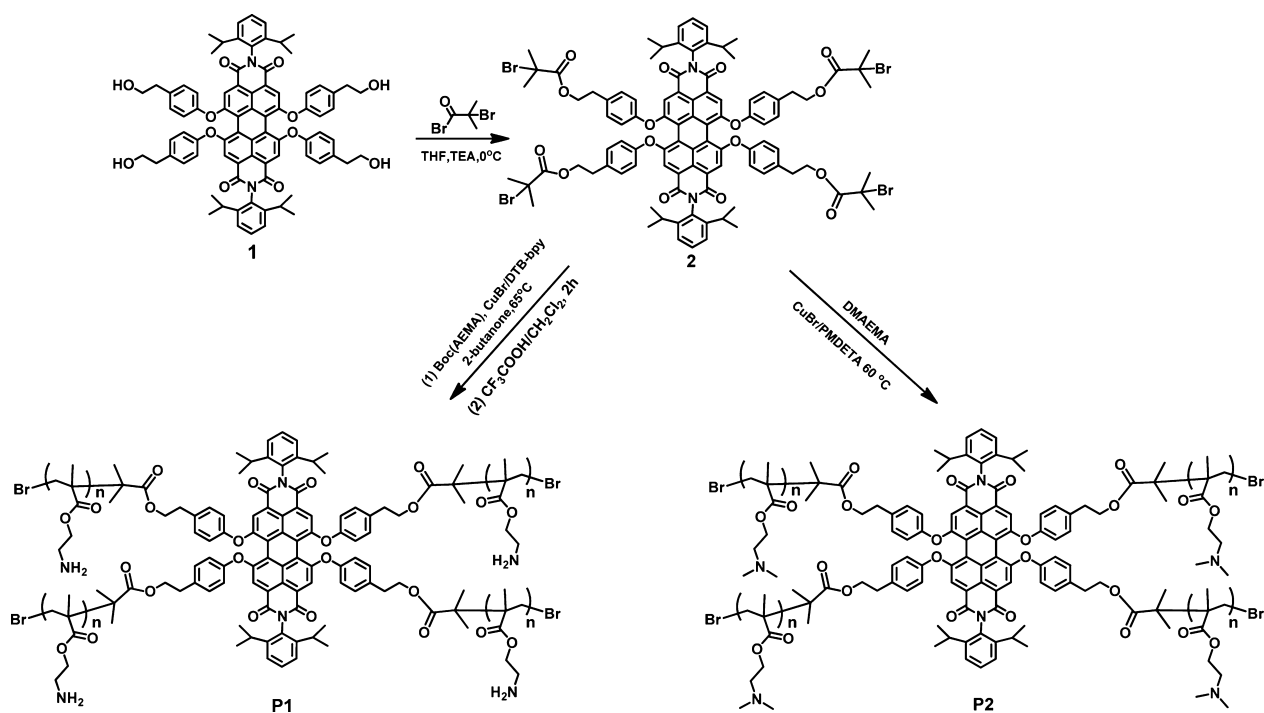
Instruments. Gel permeation chromatography (GPC) analyses were performed in DMF with a Waters 515 pump and Waters 410 differential refractometer using PSS columns (Styrogel 10⁵, 10³, 10² Å) in DMF as an eluent at 30 °C at a flow rate of 1 mL/min. The column system was calibrated with linear PMMA standards. All proton nuclear

magnetic resonance (NMR) spectra were determined on a “Bruker-Spectrospin” instrument (400 MHz) at room temperature. Matrix-assisted laser-desorption ionization time-of-flight mass spectrometry (MALDI-TOF MS) was determined on a Bruker Daltonics Inc. BIFLEX III MALDI-TOF mass spectrometer. The UV spectroscopy was determined by UV–visible spectrophotometer (Australia, GBC Cintra-20 spectro-photometer). The scan wavelength range was 200–900 nm; scanning frequency was 1000 nm/min, and spectral resolution was 0.427 nm. The corrected fluorescence spectroscopic studies were performed on a fluorescence spectrophotometer (Horiba Jobin Yvon FluoroMax-4 NIR, NJ, USA) at room temperature. The pH measurements were carried out using a pH meter (Mettler Toledo S40K), which was calibrated with pH 4.0 and pH 7.0 buffers before use.

Synthesis of Macroinitiator 2. The synthesis of macroinitiator **2** has been described in previous publications.³⁷ Typically, 2-bromoisobutryl bromide (BIBBr, 3.2 mL, 25.6 mmol) was added dropwise to a mixture of **1** (800 mg, 0.64 mmol) and TEA (3.6 mL, 25.6 mmol) in THF (40.0 mL) at 0 °C. Afterward, the mixture was allowed to stir for 3 days at room temperature. Then, the solution was washed with 50.0 mL of saturated brine and 50.0 mL of deionized water twice. The organic layer was separated and dried over anhydrous MgSO₄. After filtration, the solution was concentrated, and the crude product was purified by column chromatography (SiO₂) using CH₂Cl₂ as the eluent. Yield: 1.06 g (90%). The final product was dried in a vacuum to a constant weight. ¹H NMR (400 MHz, CDCl₃, 25 °C): δ 8.22 (s, 4 H, perylene), 7.43 (t, 2 H, Ph-H), 7.28 (d, 4 H, Ph-H), 7.17 (d, 8 H, Ph-H), 6.89 (d, 8 H, Ph-H), 4.34 (t, 8 H, –CH₂O(C=O)–), 2.94 (t, 8 H, PhCH₂–), 2.67 (h, 4 H, CH isopropyl), 1.90 (s, 24H, CH₃ isobutyrate), 1.10 (d, 24H, CH₃ isopropyl). MS (MALDI-TOF, *m/z*) Calc. for C₉₆H₃₄Br₄N₂O₁₆: 1846.33. Found: 1847.5 (M+H⁺), 1869.5 (M+Na⁺), 1885.5 (M+K⁺).

Synthesis of P1. A Schlenk tube was charged with initiator **2** (40 mg, 0.022 mmol, 1 equiv), (Boc)AEMA (2.0 g, 8.8 mmol, 4 × 100 equiv), CuBr (12.5 mg, 0.088 mmol, 4 × 1 equiv), and dry 2-butanone (2.0 mL). The tube was degassed by three freeze–pump–thaw cycles, and then DTB-bipy (11.8 mg, 0.044 mmol, 4 × 2 equiv) was added. After being stirred for 10 min to ensure the catalyst completely formed a complex, the polymerization was carried out under a N₂ atmosphere

Scheme 2. Synthesis Route of (PAEMA, P1) and (PDMAEMA, P2)



at 60 °C. After a defined reaction time, the polymerization was stopped by cooling with liquid nitrogen. The mixture was diluted with 10 mL of dichloromethane and passed through an alumina column to eliminate the used copper salts. After being concentrated by rotovap, the solution was poured into excess methanol/water ($v/v = 1:1$) to precipitate the polymer, and the crude product was precipitated in methanol/water ($v/v = 1:1$) another three times. After drying in a vacuum oven overnight at room temperature, the product (594 mg, yield: 29.7%) was obtained as a red solid.

The solid was dissolved in dichloromethane (20 mL) in a 100 mL round-bottomed flask, and then CF_3COOH (20 mL) was added. The mixture was stirred for 2 h at room temperature. After the solvent evaporated, the residue was dissolved in methanol (10 mL). After being reprecipitated in diethyl ether three times and dried under a vacuum, the product **P1** (312 mg, yield: 93.2%) was obtained as a red solid.

Synthesis of P2. A reaction tube was charged with initiator **2** (10 mg, 5.4×10^{-3} mmol, 1 equiv), DMAEMA (339 mg, 2.16 mmol, 4×100 equiv), and dry THF (2.0 mL). The tube was degassed by three freeze–pump–thaw cycles, and then PMDETA (15 mg, 0.216 mmol, 4×2 equiv) and CuBr (3.1 mg, 2.2×10^{-2} mmol, 4×1 equiv) were added to the reaction tube. After being stirred for 10 min at room temperature, the polymerization was carried out under a N_2 atmosphere at 60 °C for 24 h. After being quenched by liquid nitrogen, the solution passed an alumina column to eliminate the used copper salt. Then, the solution was poured into excess *n*-heptane to precipitate the polymer. The precipitate was dissolved in dichloromethane and precipitated again in *n*-heptane. After drying in a vacuum oven overnight at room temperature, **P2** (97 mg, Yield: 28.6%) was obtained as a red powder.

Optical Property Assay of P1 and P2. **P1** and **P2** were dissolved in deionized water at various concentrations. Their absorbance and fluorescence spectra were performed to examine their optical properties in water.

Preparation of Polymer/DNA Complexes. The purity and concentration of the purified DNA were determined by absorption at 260 and 280 nm and by agarose gel electrophoresis. N/P ratios are expressed as molar ratios of nitrogen (N) in **P1** or **P2** to phosphate (P) in DNA. An average mass weight of 325 per phosphate group of DNA was assumed. All polymer/DNA complexes were formed by mixing equal volumes of polymers and DNA solutions to achieve the desired N/P ratio. Each mixture was vortexed and incubated for 30 min at room temperature.

Acid–Base Titration. The buffering capacity of the synthesized polymers from pH 5.1 to 7.4 was determined by acid–base titration. **P1** and **P2** with 10 mmol of amine groups were dissolved in 10 mL of 0.1 M NaCl. The pH value of the polymer solution was set at 2.5 with 1 M HCl, and then the solution was titrated with 0.001 M NaOH solution by adding 0.1 mL of NaOH solution each time. The 0.1 M NaCl was also examined using the same method as a control.

Zeta Potential and Particle Size Measurements. The zeta potential (ζ) and particle size of the polymers and polymer/DNA complexes were measured in triplicate at 25 °C with a Zetasizer Nano ZS (Malvern Instruments, Southborough, MA), which is based on electrophoretic light scattering.

Agarose Gel Electrophoresis Assay. The DNA binding capability of polymer was detected by agarose gel electrophoresis assay. The polymer/DNA complexes with different N/P ratios were loaded on a 1.5% agarose gel, and electrophoresis was performed at 80 V for 30 min in a TAE buffer solution (40 mM Tris–HCl, 1.5% acetic acid, and 1 mM EDTA). The retardation of DNA was imaged by an ethidium bromide stain for 10 min after electrophoresis. The photograph was acquired under UV light (ChamGel 5000, 365 nm).

Cell Cultures. S2 cells were cultured in Schneider's Drosophila Medium (Sigma) supplemented with 10% fetal bovine serum (FBS), penicillin (100 unit/mL), and streptomycin (100 $\mu\text{g}/\text{mL}$) at 25 °C. Confluent cells were subcultured once every 3 days according to standard method.

Cell Viability Assay. Cell viability assay was evaluated by the Tali viability kit–Dead Cell Green (Invitrogen, Catalog A10787) which

marked the dead cells with green fluorescence. The fluorescent dye (Dead Cell Green) in this kit can stain the nucleic acid of dead cells, but not the live cells. S2 cells were seeded into 35 \times 35 mm cell culture dishes at a seeding density of 2.5×10^5 cells per well. After seeding for 6 h, the S2 cells were stuck to the bottoms of the dishes. **P1**, **P2**, or PEI (25 kDa) with gradient concentrations were added into different dishes, respectively. After 48 h, the old culture medium was replaced with fresh medium mixed with 1% Dead Cell Green for 30 min. The quantitative calculation of apoptotic and normal cells was performed through a fluorescent microscope (EVOS f1, AMG).

Cellular Uptake. The cellular uptake experiment was performed in a 35 mm \times 35 mm cell culture dish, 2.5×10^5 cells per well. After 6 h of cell seeding, **P1** and **P2** were added into the cell culture dish, respectively. Cellular uptake was imaged under a fluorescence microscope. The fluorescence intensity of the internalized **P1** or **P2** was calculated by an Image-J Program.

Gene Delivery Assay. Gene delivery efficiencies of **P1** and **P2** were analyzed using S2 cells incubated in the culture medium with 10% FBS. Carrier/DNA complexes at different N/P ratios of 4:1, 8:1, 16:1, and 32:1 were prepared by mixing carrier with DNA (21 bp, 100 μM) at room temperature for 15 min. The DNA was premixed with 30 μM CXR Reference Dye (Promega, Catalog C5411) for subsequent fluorescence detection. After 6 h of cell seeding, when cell density is about 2.5×10^5 cells per well, the carrier/DNA complexes at a certain N/P ratio were added into the cell dish to incubate the S2 cells. Then, the fluorescence of DNA transported into cells was detected by fluorescent microscopy every 12 h. Quantitative fluorescence intensity of DNA in S2 cells was measured by the Image-J Program. PEI (25 kDa)/DNA complexes were employed as a control.

RESULTS AND DISCUSSION

Synthesis of P1 and P2. According to the literature,³⁷ macroinitiator **2** was successfully synthesized based on PDI fluorophore. The structural characterization can be found in Figure 1 and Figure S1. PDI-cored star P(Boc)AEMA was

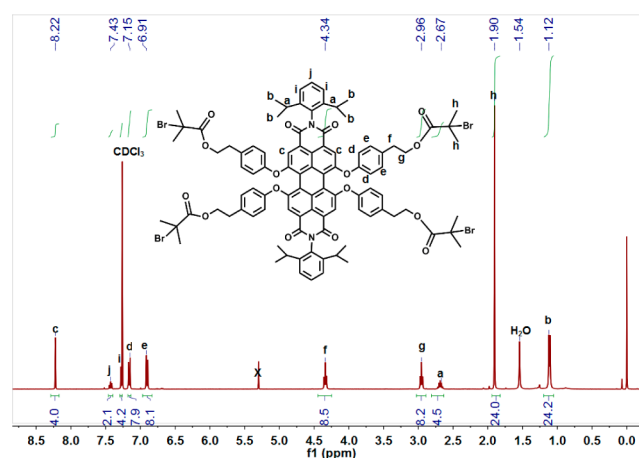


Figure 1. ^1H NMR spectrum of **2** in CDCl_3 .

synthesized via ATRP using Boc(AEMA) as the monomer and **2** as the macroinitiator. The following deprotection gave the target PDI-cored star polymer **P1** (PAEMA) bearing primary amines. **P2** (PDMAEMA) was synthesized in a single step via ATRP. The repeat units in each arm of **P1** and **P2** were about 30, which were calculated by ^1H NMR spectra of reaction mixtures. Figures 2 and 3 show the ^1H NMR spectra of the star polymers **P1** and **P2**, respectively. GPC data show that both **P1** and **P2** have low molecular weight distributions ($M_w/M_n < 1.5$, Table 1 and Figure S2).

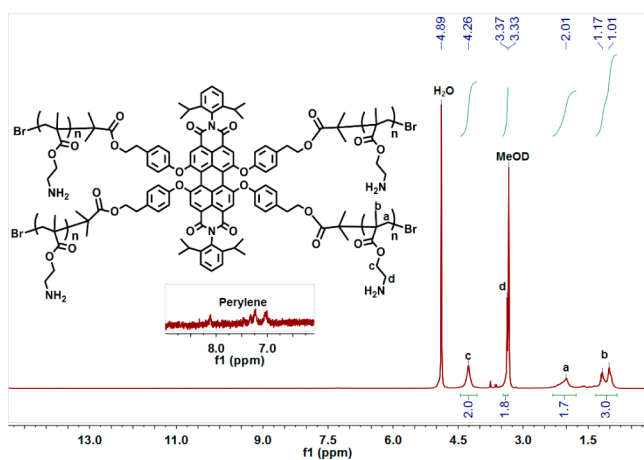


Figure 2. ^1H NMR spectrum of P1 in CD_3OD .

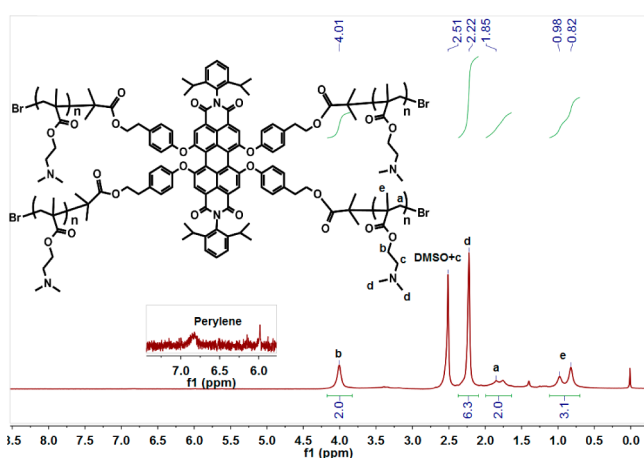


Figure 3. ^1H NMR spectrum of P2 in DMSO.

Table 1. Polymerization Data of P1 and P2

polymers	r.u. ^a	M_{NMR}^b (g/mol)	$M_{n,\text{GPC}}$ (g/mol)	$M_{w,\text{GPC}}$	pdi ^c
P1	30	17300	14500	16000	1.10
P2	30	20700	20100	25700	1.28

^aRepeat units of each arm. ^bCalculated from ^1H NMR spectra. ^cpdi = M_w/M_n .

Optical Properties of P1 and P2. P1 and P2 were dissolved in deionized water to obtain aqueous solutions with various concentrations. The aggregation behavior of P1 and P2 was studied by concentration-dependent absorption spectroscopy (Figure 4). The absorption bands of P1 and P2 at 450, 540, and 580 nm were similar to the previous reported PDI cored dendritic macromolecules.³⁸ The absorption spectra of P1 and P2 maintained the same shape and maximum at the varied concentrations. Meanwhile, linear concentration-dependent absorption is observed in aqueous solutions of P1 and P2 (Figure 4, inset). The results suggest that both P1 and P2 stay in a single-molecule state in the aqueous solutions over the whole concentration range studied. The fluorescence spectra at an excitation wavelength of 540 nm were also investigated. The characteristic emission exhibits a peak at 622 nm, which is far away from the wavelength of cell autofluorescence. The fluorescence quantum yield (Φ_f) was measured at room temperature using Cresyl Violet in methanol (the standard value is 0.54) as reference.³⁹ Φ_f 's of P1 and P2 in water are 0.14

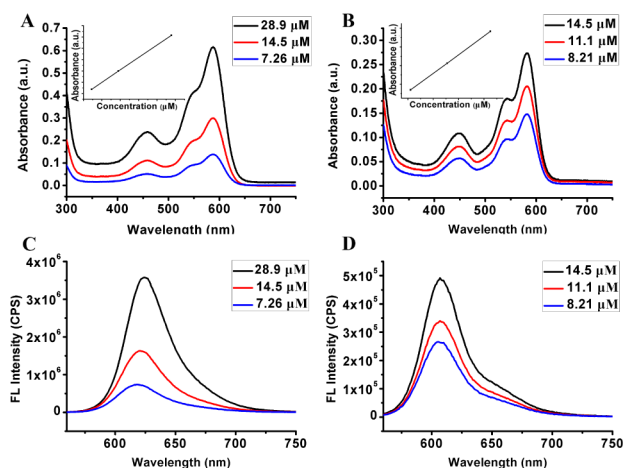


Figure 4. Absorbance spectra of (A) P1 and (B) P2 at different concentrations; fluorescence spectra of (C) P1 and (D) P2 at different concentrations ($E_x = 540$ nm). Inset: concentration dependence of absorbance intensity ($E_{\text{max}} = 580$ nm).

and 0.06, respectively. When forming complexes with DNA, their Φ_f values are increased to 0.16 (P1/DNA) and 0.07 (P2/DNA), respectively. The optical intensities of the two star polymers in water remain unchanged after being exposed to natural light for 2 weeks, indicating their high photostability. The optical properties suggest that the star polymers P1 and P2 are suitable for biological applications.

Acid–Base Titration. Polycations are assumed to induce facilitated endosomal escape due to the uptake of protons by the amino groups when the pH in the endosomes decreases from 7.4 to 5.1 (proton sponge hypothesis).⁴⁰ According to the previous reports, better buffering capacity of polycations at low pH will contribute to higher transfection efficiency of polycation/DNA complexes.^{41–43} Thus, acid–base titrations were used to evaluate the buffering capacity (Figure 5). The

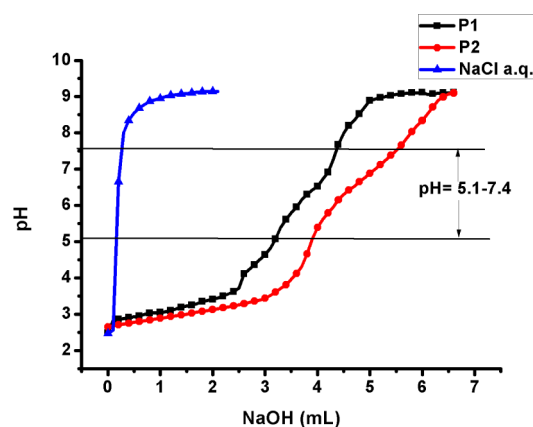


Figure 5. Acid–base titration curves. The solutions of P1 and P2 with the same concentration of amino groups (5×10^{-3} mol/L) in aqueous NaCl (0.1 mol/L, pH 2.5, adjusted with HCl) was titrated with NaOH (1×10^{-3} mol/L).

buffering capacity was determined as millimoles (mmol) of OH^- per mmol of amines of polymer. To increase the pH of the polymer solution from 5.1 to 7.4, P1 and P2 need to bind 0.20 and 0.32 mmol OH^- per mmol of amines of polymer, respectively, which demonstrates that P2 can bind more OH^-

than P1 in this pH range. In other words, P2 has a higher buffering capacity than P1.

Zeta Potential and Particle Size Measurements. The DNA condensation capabilities of P1 and P2 can be measured by their zeta potentials and particle sizes. The data are shown in Table 2. As expected, they are positively charged before and

Table 2. Particle Sizes and Zeta Potentials of P1, P2, and Their Complexes with DNA at N/P = 10

	P1	P1/DNA	P2	P2/DNA
size (nm)	26.5	145.6	33.4	156.8
Z potential (mv)	37.8	24.0	56.5	13.6

after being complexed with DNA at N/P = 10. Particularly, P2 had a higher zeta potential (56.5 mV) than P1 (37.8 mV). After the addition of negatively charged DNA, the zeta potential of the P2/DNA complex (13.6 mV) sharply decreased and was even lower than that of the P1/DNA complex (24.0 mV). This could be explained by the high DNA-binding ability of P2.⁴⁴

Meanwhile, P1 and P2 have relatively small hydrodynamic diameters (<50 nm). When complexed with DNA, both P1 and P2 formed small cationic nanoparticles (<200 nm). The appropriate sizes of complexes below 200 nm imply that the nanoparticles are in suitable size for cell uptake.^{45,46}

Agarose Gel Electrophoresis Assay. An agarose gel retardation assay was performed to study the stability of polymer/DNA complexes at various N/P ratios. As shown in Figure 6, the band's intensity of the migrated DNA gradually

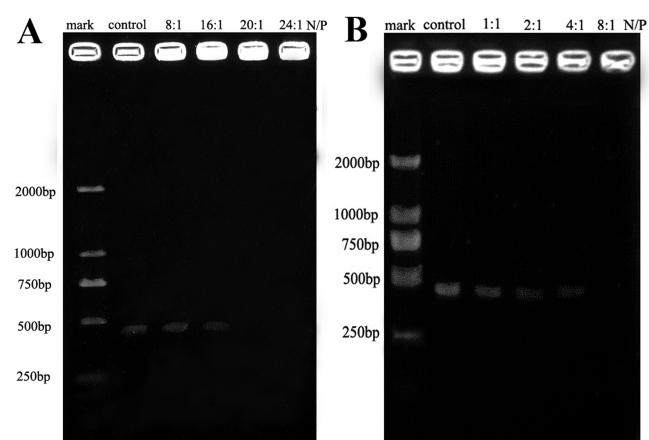


Figure 6. Gel electrophoresis assay of DNA retardation by (A) P1 and (B) P2 at various N/P ratios.

decreased with increasing N/P ratios. The complexes were completely retarded at ratios higher than 20 (P1) or 8 (P2). Both P1 and P2 have acceptable abilities for condensing DNA. P2 showed better performance than P1, which is consistent with the zeta potential results.

Cell Viability and Cellular Uptake Assay. Low cytotoxicity is a vital parameter for ideal gene carriers. We tested the cytotoxicity of the two polymers and PEI (25 kDa) at various concentrations by cell viability assays. P1 and P2 displayed much higher cell viabilities than PEI at all the tested concentrations (Figure 7). These data suggest that the polymers have good biocompatibility.

Taking the advantage of strong fluorescence of the star polymers P1 and P2, we can conveniently trace the

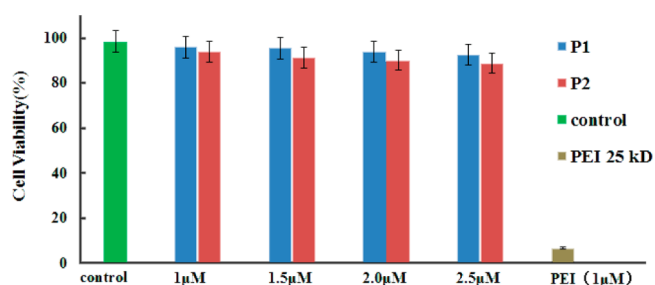


Figure 7. *In vitro* cytotoxicity assay of P1, P2, and PEI (25 kDa) at different concentrations.

fluorescence distribution of P1 and P2 (Figure S4) in cells under a fluorescence microscope. The star polymers were incubated with cells at various concentrations and incubation times. Their fluorescence intensities of the internalized P1 and P2 were calculated by an Image-J Program and are shown in Figures S6 and S7. The cellular uptake experiments indicate that both P1 and P2 can successfully enter the live cells within a short incubation time. The fluorescence intensity of P2 in the cells is higher than that of P1 at the same incubation time, demonstrating that P2 is faster than P1 to be internalized into cells.

***In Vitro* Gene Transfection Assay.** In addition to low cytotoxicity, high gene delivery efficiency is also a key parameter for ideal gene vectors. In order to assess the ability of gene delivery, S2 cells were treated with P1/DNA and P2/DNA complexes, respectively. PEI/DNA complexes was employed as a control. Taking the advantage of strong fluorescence of our polymers, fluorescence microscopy was used to assay the efficiency of cellular uptake. Except for PEI (Figure S5), both P1 (Figure 8, A–A'') and P2 (Figure 8, B–B'') were able to deliver DNA into cells at high efficiency as demonstrated by the fluorescence of polymers (red) and CXR-labeled DNA (blue; Figure 8).

To reveal the details of DNA delivery efficiency, gene transfection efficiency of P1 and P2 was tested at various N/P ratios ranging from 1:1 to 32:1 as shown in Figure 9. The fluorescence of delivered DNA can be detected at a low N/P ratio of 4:1. The fluorescence intensity increased with the N/P

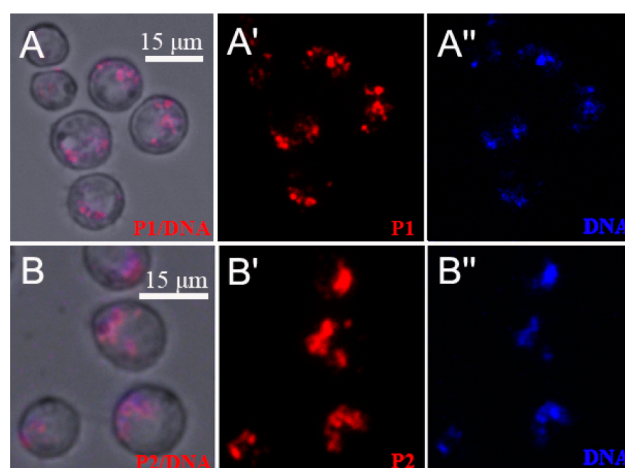


Figure 8. Fluorescence images of (A) P1/DNA and (B) P2/DNA complexes internalized into cells after 48 h incubation (N/P = 20). A' and B' are fluorescence images of P1 and P2 (red). A'' and B'' are fluorescence images of DNA labeled with CXR Reference Dye (blue).

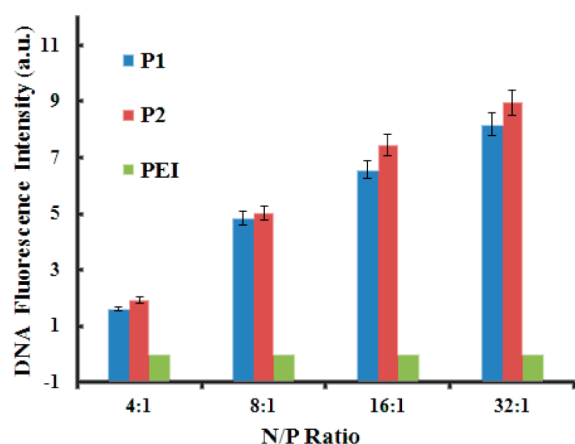


Figure 9. Fluorescence intensities of **P1**, **P2**, and **PEI** (25 kDa) delivered CXR-labeled DNA in cells (60 h incubation) at different N/P ratios.

ratio and reached the highest at the ratio of 32:1. In the control experiment, the fluorescence intensity of DNA delivered by **PEI** was too low to be detected at the same imaging settings at all the tested N/P ratios even for 32:1 (Figure S5). The results demonstrated that **P1** and **P2** are good gene carriers. **P2** showed better performance than **P1** at all the tested N/P ratios. To further compare the gene delivery efficiency between **P1** and **P2**, treatments under different incubating durations were performed (Figure 10). The fluorescence intensities of CXR-

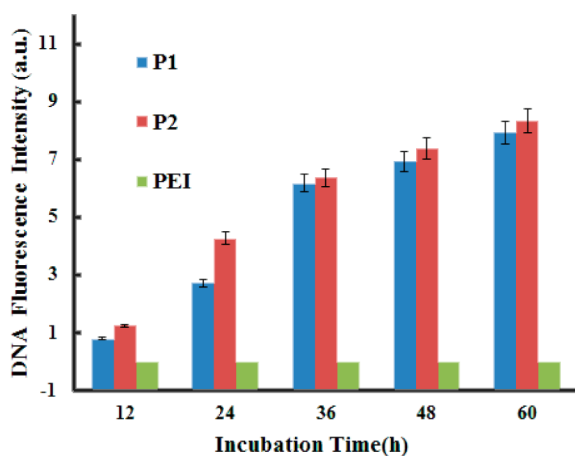


Figure 10. Fluorescence intensities of **P1**, **P2**, and **PEI** (25 kDa) delivered CXR-labeled DNA in cells (N/P = 20) after different incubation time.

labeled DNA delivered by **P2** are always higher than those delivered by **P1**, which is consistent with the above results obtained from acid–base titration.⁴² The higher transfection efficiency makes **P2** a better gene vector than **P1**.

CONCLUSIONS

In summary, two efficient gene vectors, **P1** and **P2**, were successfully synthesized using ATRP strategy. Both the star polymers have good water solubilities and emit strong fluorescence in aqueous solutions due to the PDI fluorophore. The red fluorescence emitted by the polymers can be detected in the live cells under a fluorescence microscope. The *in vitro* gene delivery assay demonstrated that both **P1** and **P2** had low cell toxicity and high gene delivery efficiency compared with

PEI (25 kDa). Unlike the PDI-cored dendrimers with similar efficacy, the PDI-cored star polycations are easy for mass production. **P2** bearing tertiary amines has stronger buffering ability than **P1** bearing primary amines. Moreover, **P2** shows higher capacity for gene delivery than **P1**. This kind of fluorescent star polycation may have good potential to be explored as a general tool for *in vivo* gene transfection. Future research will focus on this application.

ASSOCIATED CONTENT

Supporting Information

Experimental procedures, characterization of the macromolecules, supporting figures, and text. This material is available free of charge via the Internet at <http://pubs.acs.org>.

AUTHOR INFORMATION

Corresponding Authors

*E-mail: yinmz@mail.buct.edu.cn

*E-mail: shenjie@cau.edu.cn

Notes

The authors declare no competing financial interest.

ACKNOWLEDGMENTS

This work was financially supported by the 973 program (2013CB127603), the National Science Foundation of China (21174012, 51103008, and 51221002), and the Beijing Natural Science Foundation (2142026).

REFERENCES

- (1) Nguyen, T.-T.-T.; Türp, D.; Wang, D.; Nölscher, B.; Laquai, F. d. r.; Müllen, K. A Fluorescent, Shape-Persistent Dendritic Host with Photoswitchable Guest Encapsulation and Intramolecular Energy Transfer. *J. Am. Chem. Soc.* **2011**, *133*, 11194–11204.
- (2) Oesterling, I.; Müllen, K. Multichromophoric Polyphenylene Dendrimers: Toward Brilliant Light Emitters with an Increased Number of Fluorophores. *J. Am. Chem. Soc.* **2007**, *129*, 4595–4605.
- (3) Qu, J.; Zhang, J.; Grimsdale, A. C.; Müllen, K.; Jaiser, F.; Yang, X.; Neher, D. Dendronized Perylene Diimide Emitters: Synthesis, Luminescence, and Electron and Energy Transfer Studies. *Macromolecules* **2004**, *37*, 8297–8306.
- (4) Qu, J. Q.; Kohl, C.; Pottek, M.; Müllen, K. Ionic Perylenetetra-carboxydiimides: Highly Fluorescent and Water-Soluble Dyes for Biolabeling. *Angew. Chem., Int. Ed.* **2004**, *43*, 1528–1531.
- (5) Peneva, K.; Mihov, G.; Nolde, F.; Rocha, S.; Hotta, J. i.; Braeckmans, K.; Hofkens, J.; Uji-i, H.; Herrmann, A.; Müllen, K. Water-Soluble Monofunctional Perylene and Terrylene Dyes: Powerful Labels for Single-Enzyme Tracking. *Angew. Chem.* **2008**, *120*, 3420–3423.
- (6) Peneva, K.; Mihov, G.; Herrmann, A.; Zarrabi, N.; Börsch, M.; Duncan, T. M.; Müllen, K. Exploiting the Nitrotriacetic Acid Moiety for Biolabeling with Ultrastable Perylene Dyes. *J. Am. Chem. Soc.* **2008**, *130*, 5398–5399.
- (7) Cordes, T.; Vogelsang, J.; Anaya, M.; Spagnuolo, C.; Gietl, A.; Summerer, W.; Herrmann, A.; Müllen, K.; Tinnefeld, P. Single-Molecule Redox Blinking of Perylene Diimide Derivatives in Water. *J. Am. Chem. Soc.* **2010**, *132*, 2404–2409.
- (8) Yin, M.; Kuhlmann, C. R.; Sorokina, K.; Li, C.; Mihov, G.; Pietrowski, E.; Koynov, K.; Klapper, M.; Luhmann, H. J.; Weil, T. Novel Fluorescent Core–Shell Nanocontainers for Cell Membrane Transport. *Biomacromolecules* **2008**, *9*, 1381–1389.
- (9) Zhang, X.; Zhang, X.; Tao, L.; Chi, Z.; Xu, J.; Wei, Y. Aggregation Induced Emission-Based Fluorescent Nanoparticles: Fabrication Methodologies and Biomedical Applications. *J. Mater. Chem. B* **2014**, *2*, 4398–4414.
- (10) Zhang, X.; Zhang, X.; Yang, B.; Hui, J.; Liu, M.; Chi, Z.; Liu, S.; Xu, J.; Wei, Y. Facile Preparation and Cell Imaging Applications of

Fluorescent Organic Nanoparticles That Combine AIE Dye and Ring-Opening Polymerization. *Polym. Chem.* **2014**, *5*, 318–322.

(11) Zhang, X.; Zhang, X.; Yang, B.; Zhang, Y.; Wei, Y. A New Class of Red Fluorescent Organic Nanoparticles: Noncovalent Fabrication and Cell Imaging Applications. *ACS Appl. Mater. Interfaces* **2014**, *6*, 3600–3606.

(12) Chen, M.; Yin, M. Design and Development of Fluorescent Nanostructures for Bioimaging. *Prog. Polym. Sci.* **2014**, *39*, 365–395.

(13) Yin, M.; Shen, J.; Gropeanu, R.; Pflugfelder, G. O.; Weil, T.; Müllen, K. Fluorescent Core/Shell Nanoparticles for Specific Cell-Nucleus Staining. *Small* **2008**, *4*, 894–898.

(14) Yin, M.; Shen, J.; Pflugfelder, G. O.; Müllen, K. A Fluorescent Core-Shell Dendritic Macromolecule Specifically Stains the Extracellular Matrix. *J. Am. Chem. Soc.* **2008**, *130*, 7806–7807.

(15) Gao, B.; Li, H.; Liu, H.; Zhang, L.; Bai, Q.; Ba, X. Water-Soluble and Fluorescent Dendritic Perylene Bisimides for Live-Cell Imaging. *Chem. Commun.* **2011**, *47*, 3894–3896.

(16) Liu, W.; Wei, J.; Chen, Y.; Huo, P.; Wei, Y. Electrospinning of Poly (L-Lactide) Nanofibers Encapsulated with Water-Soluble Fullerenes for Bioimaging Application. *ACS Appl. Mater. Interfaces* **2013**, *5*, 680–685.

(17) Yang, S. K.; Shi, X.; Park, S.; Doganay, S.; Ha, T.; Zimmerman, S. C. Monovalent, Clickable, Uncharged, Water-Soluble Perylenediimide-Cored Dendrimers for Target-Specific Fluorescent Biolabeling. *J. Am. Chem. Soc.* **2011**, *133*, 9964–9967.

(18) Liu, K.; Xu, Z.; Yin, M.; Yang, W.; He, B.; Wei, W.; Shen, J. A Multifunctional Perylenediimide Derivative Can Be Used as a Recyclable Specific Hg²⁺ Ion Sensor and an Efficient DNA Delivery Carrier. *J. Mater. Chem. B* **2014**, *2*, 2093–2096.

(19) Xu, Z.; He, B.; Wei, W.; Liu, K.; Yin, M.; Yang, W.; Shen, J. Highly Water-Soluble Perylenediimide-Cored Poly(Amido Amine) Vector for Efficient Gene Transfection. *J. Mater. Chem. B* **2014**, *2*, 3079–3086.

(20) Xu, Z.; He, B.; Shen, J.; Yang, W.; Yin, M. Fluorescent Water-Soluble Perylenediimide-Cored Cationic Dendrimers: Synthesis, Optical Properties, and Cell Uptake. *Chem. Commun.* **2013**, *49*, 3646–3648.

(21) Wang, F.; Rauh, R. D.; Rose, T. L. An Electrically Conducting Star Polymer. *J. Am. Chem. Soc.* **1997**, *119*, 11106–11107.

(22) Gao, H.; Matyjaszewski, K. Low-Polydispersity Star Polymers with Core Functionality by Cross-Linking Macromonomers Using Functional ATRP Initiators. *Macromolecules* **2007**, *40*, 399–401.

(23) Omer, K. M.; Ku, S.-Y.; Chen, Y.-C.; Wong, K.-T.; Bard, A. J. Electrochemical Behavior and Electrogenerated Chemiluminescence of Star-Shaped D-A Compounds with a 1, 3, 5-Triazine Core and Substituted Fluorene Arms. *J. Am. Chem. Soc.* **2010**, *132*, 10944–10952.

(24) Matyjaszewski, K.; Xia, J. Atom Transfer Radical Polymerization. *Chem. Rev.* **2001**, *101*, 2921–2990.

(25) Rodionov, V.; Gao, H.; Scroggins, S.; Unruh, D. A.; Avestro, A.-J.; Fréchet, J. M. Easy Access to a Family of Polymer Catalysts from Modular Star Polymers. *J. Am. Chem. Soc.* **2010**, *132*, 2570–2572.

(26) Yin, M.; Kang, N.; Cui, G.; Liu, Z.; Wang, F.; Yang, W.; Klapper, M.; Müllen, K. Synthesis, Electrochemical Properties and Self-Assembly of a Proton-Conducting Core-Shell Macromolecule. *Chem.—Eur. J.* **2012**, *18*, 2239–2243.

(27) Blaese, R. M.; Culver, K. W.; Miller, A. D.; Carter, C. S.; Fleisher, T.; Clerici, M.; Shearer, G.; Chang, L.; Chiang, Y.; Tolstoshev, P.; Greenblatt, J. J.; Rosenberg, S. A.; Klein, H.; Berger, M.; Mullen, C. A.; Ramsey, W. J.; Muul, L.; Morgan, R. A.; Anderson, W. F. T Lymphocyte-Directed Gene Therapy for ADA-Scid: Initial Trial Results after 4 Years. *Science (New York, N.Y.)* **1995**, *270*, 475–80.

(28) Khuri, F. R.; Nemunaitis, J.; Ganly, I.; Arseneau, J.; Tannock, I. F.; Romel, L.; Gore, M.; Ironside, J.; MacDougall, R. H.; Heise, C.; Randlev, B.; Gillenwater, A. M.; Brusco, P.; Kaye, S. B.; Hong, W. K.; Kirn, D. H. A Controlled Trial of Intratumoral Onyx-015, a Selectively-Replicating Adenovirus, in Combination with Cisplatin

and 5-Fluorouracil in Patients with Recurrent Head and Neck Cancer. *Nat. Med.* **2000**, *6*, 879–85.

(29) Davis, M. E. The First Targeted Delivery of Sirna in Humans Via a Self-Assembling, Cyclodextrin Polymer-Based Nanoparticle: From Concept to Clinic. *Mol. Pharmaceutics* **2009**, *6*, 659–668.

(30) Cao, Z.; Liu, W.; Liang, D.; Guo, G.; Zhang, J. Design of Poly (Vinylidiaminotriazine)-Based Nonviral Vectors Via Specific Hydrogen Bonding with Nucleic Acid Base Pairs. *Adv. Funct. Mater.* **2007**, *17*, 246–252.

(31) Boussif, O.; Lezoualc'h, F.; Zanta, M. A.; Mergny, M. D.; Scherman, D.; Demeneix, B.; Behr, J.-P. A Versatile Vector for Gene and Oligonucleotide Transfer into Cells in Culture and in Vivo: Polyethylenimine. *Proc. Natl. Acad. Sci. U. S. A.* **1995**, *92*, 7297–7301.

(32) Lee, Y.; Mo, H.; Koo, H.; Park, J.-Y.; Cho, M. Y.; Jin, G.-w.; Park, J.-S. Visualization of the Degradation of a Disulfide Polymer, Linear Poly (Ethylenimine Sulfide), for Gene Delivery. *Bioconjugate Chem.* **2007**, *18*, 13–18.

(33) Zhang, P.; Yang, J.; Li, W.; Wang, W.; Liu, C.; Griffith, M.; Liu, W. Cationic Polymer Brush Grafted-Nanodiamond Via Atom Transfer Radical Polymerization for Enhanced Gene Delivery and Bioimaging. *J. Mater. Chem.* **2011**, *21*, 7755–7764.

(34) Jiang, X.; Lok, M. C.; Hennink, W. E. Degradable-Brushed PHEMA-PDMAEMA Synthesized Via ATRP and Click Chemistry for Gene Delivery. *Bioconjugate Chem.* **2007**, *18*, 2077–2084.

(35) Dubruel, P.; Christiaens, B.; Rosseneu, M.; Vandekerckhove, J.; Grooten, J.; Goossens, V.; Schacht, E. Buffering Properties of Cationic Polymethacrylates Are Not the Only Key to Successful Gene Delivery. *Biomacromolecules* **2004**, *5*, 379–388.

(36) Klok, H. A.; Becker, S.; Schuch, F.; Pakula, T.; Müllen, K. Synthesis and Solid State Properties of Novel Fluorescent Polyester Star Polymers. *Macromol. Biosci.* **2003**, *3*, 729–741.

(37) Klok, H. A.; Becker, S.; Schuch, F.; Pakula, T.; Müllen, K. Fluorescent Star-Shaped Polystyrenes: “Core-First” Synthesis from Perylene-Based ATRP Initiators and Dynamic Mechanical Solid-State Properties. *Macromol. Chem. Phys.* **2002**, *203*, 1106–1113.

(38) You, S.; Cai, Q.; Müllen, K.; Yang, W.; Yin, M. pH-Sensitive Unimolecular Fluorescent Polymeric Micelles: From Volume Phase Transition to Optical Response. *Chem. Commun.* **2014**, *50*, 823–825.

(39) Qu, J.; Kohl, C.; Pottek, M.; Müllen, K. Ionic Perylene-tetracarboxydiimides: Highly Fluorescent and Water-Soluble Dyes for Biolabeling. *Angew. Chem.* **2004**, *116*, 1554–1557.

(40) Lin, C.; Blaauboer, C.-J.; Timoneda, M. M.; Lok, M. C.; van Steenberg, M.; Hennink, W. E.; Zhong, Z.; Feijen, J.; Engbersen, J. F. Bio-reducible Poly(amido amine)s with Oligoamine Side Chains: Synthesis, Characterization, and Structural Effects on Gene Delivery. *J. Controlled Release* **2008**, *126*, 166–174.

(41) Zhong, Z.; Feijen, J.; Lok, M. C.; Hennink, W. E.; Christensen, L. V.; Yockman, J. W.; Kim, Y.-H.; Kim, S. W. Low Molecular Weight Linear Polyethylenimine-b-Poly(ethylene glycol)-b-Polyethylenimine Triblock Copolymers: Synthesis, Characterization, and in Vitro Gene Transfer Properties. *Biomacromolecules* **2005**, *6*, 3440–3448.

(42) Dai, F.; Sun, P.; Liu, Y.; Liu, W. Redox-Cleavable Star Cationic PDMAEMA by Arm-First Approach of ATRP as a Nonviral Vector for Gene Delivery. *Biomaterials* **2010**, *31*, 559–569.

(43) Yu, S.; Chen, J.; Dong, R.; Su, Y.; Ji, B.; Zhou, Y.; Zhu, X.; Yan, D. Enhanced Gene Transfection Efficiency of PDMAEMA by Incorporating Hydrophobic Hyperbranched Polymer Cores: Effect of Degree of Branching. *Polym. Chem.* **2012**, *3*, 3324–3329.

(44) Petersen, H.; Kunath, K.; Martin, A. L.; Stolnik, S.; Roberts, C. J.; Davies, M. C.; Kissel, T. Star-Shaped Poly (Ethylene Glycol)-Block-Polyethylenimine Copolymers Enhance DNA Condensation of Low Molecular Weight Polyethylenimines. *Biomacromolecules* **2002**, *3*, 926–936.

(45) Pu, Y.; Chang, S.; Yuan, H.; Wang, G.; He, B.; Gu, Z. The Anti-Tumor Efficiency of Poly (L-Glutamic Acid) Dendrimers with Polyhedral Oligomeric Silsesquioxane Cores. *Biomaterials* **2013**, *34*, 3658–3666.

(46) Maeda, H.; Wu, J.; Sawa, T.; Matsumura, Y.; Hori, K. Tumor Vascular Permeability and the EPR Effect in Macromolecular Therapeutics: A Review. *J. Controlled Release* **2000**, *65*, 271–284.